2

Idaho National Engineering Laboratory

Managed by the U.S. Department of Energy

EGG-FSP-10166
March 1992

TUNGSTEN ALLOY OXIDATION BEHAVIOR IN AIR AND STEAM

G. R. Smolik

EG&G Idaho

Work performed under DOE Contract No. DE-AC07-76ID01570

This document contains new concepts or the author(s) interpretation of new calculations and/or measurements; accordingly, EG&G Idaho, Inc. is required by the United States Government to include the following disclaimer:

EGG-FSP--10166

DE92 018051

Tungsten Alloy Oxidation Behavior in Air and Steam

Fusion Safety Program/Activation Products Task

Galen R. Smolik

Published March 1992

Idaho National Engineering Laboratory
EG&G Idaho, Inc.
Idaho Falls, Idaho 83415

Prepared for the
U.S. Department of Energy
Office of Energy Research
Under DOE Field Office, Idaho
Contract DE-AC07-76ID01570

ABSTRACT

This report presents oxidation rates derived from posttest evaluations of a tungsten alloy initially tested at the INEL in air and steam between 600° C and 1200° C to obtain volatilization measurements which have been previously reported[1,2]. Oxidation behavior of pure tungsten in air and environments containing water vapor is initially reviewed. The oxidation rates which we have found for the alloy in air and steam, expressed as recession rates (mm/s), are then compared with rates reported in the literature for pure tungsten. We have also used weight changes and mass balances involved in the oxidation and volatilization processes to predict oxidation reactions and estimate remnant oxide products and quantities of hydrogen formed.

Relationships for the oxidation of the tungsten alloy in air and steam, and also, hydrogen generation in steam are given based upon data extracted both from our tests and from the literature. These are the relationships recommended for fusion safety analyses based upon the current available information. Finally, a comparison of hydrogen production rates show that the three primary plasma-facing component (PFC) materials ranked in increasing order are graphite, tungsten and beryllium. Each of these materials, however, have other safety or performance features which impact PFC selection.

SUMMARY

This report gives reaction rates for a tungsten alloy in air and steam. Tungsten is a leading candidate for use in ITER PFCs (plasma facing components). These equations are important in safety analyses because they define the quantity of material which oxidizes and can potentially volatilize thus causing a distribution of activated products. They also define the amount of hydrogen produced which could be available to form explosive mixtures. The oxidation rates also provide some insight into the extent of machine damage which may occur by an air or steam intrusion.

We made posttest examinations of specimens we had originally used to obtain volatilization measurements. These examinations involved weight change and recession rate measurements. We compared the results of these examinations with information from the literature, and compiled a set of reaction rate equations that represent our knowledge to date. The oxidation rate of the tungsten alloy in air for temperatures between 700° C and 1300° C, and oxygen partial pressures from 0.0013 atm to 20.8 atm is

$$dx/dt\ (mm/s) = 0.847\ e^{-12{,}170/T}\ P_{O_2}^{\frac{1}{2}}$$

where temperature (T) is in degrees Kelvin and oxygen pressure (P_{O_2}) is expressed in atmospheres.

The recession rate equation for the tungsten alloy in steam is based on a 50% steam, 50% argon mixture, i.e., a steam pressure of 0.42 atm, and is valid for temperatures from 600° C to 1200° C:

$$dx/dt\ (mm/s) = 7.0\ e^{-15{,}600/T}$$

Hydrogen production in steam is represented by:

$$\textit{Hydrogen Generation Rate}\ (\textit{liters}\ H_2/cm^2\text{-}s) = 4.9\ e^{-15{,}600/T}$$

We compared the hydrogen generation rate of the tungsten alloy with that of two other candidate PFC materials which we have tested at the INEL, beryllium and graphite. In order of increasing hydrogen generation rates per unit area, they are graphite, tungsten, and then beryllium. The total quantity of hydrogen produced during an accident involving PFCs depends on the specific design and operating parameters. It must be kept in mind however, that there are other safety or performance features such as activation product volatilization that impact PFC material selection.

CONTENTS

Tungsten Alloy Oxidation Behavior in Air and Steam

1. INTRODUCTION

Safety hazards for a fusion machine such as the International Thermonuclear Experimental Reactor (ITER) are dominated by plasma-facing components (PFCs). The materials used for these components, of which beryllium, graphite and tungsten are the primary candidates, influence performance and safety in several ways. These materials can influence several factors including disruption tolerances, disruption severity, tritium inventory and permeation, accidental energy release, and radioactivity and toxin releases. Failure sequences can lead to intrusions of steam or air which can react with the PFCs. These oxidation reactions are of interest to fusion safety from two aspects. They define the quantity of material which oxidizes and can potentially volatilize thus causing a distribution of activated products. They also define the amount of hydrogen produced which could be available to form explosive mixtures. The oxidation rates also provide some insight into the extent of machine damage which may occur by an air or steam intrusion. These concerns are the reasons for developing the relationships for tungsten oxidation rates and hydrogen generation rates presented in this report.

2. RECOMMENDATIONS

Rates for the oxidation of the tungsten alloy in air can be represented by a relationship developed by Ong and Fassell[3,11,12]. This relationship valid for temperatures from 700°C to 1300°C and oxygen partial pressures from 0.0013 atm to 20.8 atm is represented below. Temperature (T) is in degrees Kelvin and oxygen pressure (P_{O_2}) is expressed as atmospheres.

$$dx/dt\ (mm/s) = 0.847\ e^{-12{,}170/T}\ P_{O_2}^{\frac{1}{2}}$$

Recession rates for the tungsten alloy in steam can be represented by the equation shown below which was derived from our test data. This relationship is based upon a 50% steam:50% argon mixture, i.e., a steam pressure of 0.42 atmosphere, and for temperatures from 600°C to 1200°C. Temperature is in degrees Kelvin.

$$dx/dt\ (mm/s) = 7.0\ e^{-15{,}600/T}$$

Hydrogen production in steam can be estimated from the above equation as follows:

$$\textit{Hydrogen Generation Rate}\ (\textit{liters}\ H_2/cm^2\text{-}s) = 4.9\ e^{-15{,}600/T}$$

3. REVIEW OF OXIDATION PROCESSES

Tungsten exposed in high temperature air, or an oxygen-containing environment, exhibits behavior which changes from parabolic at temperatures below 700° C to para-linear above 700° C. Para-linear behavior is when oxygen uptake is initially parabolic but later becomes linear. A compact scale which restricts oxygen ion diffusion initially forms at low temperatures. Some[4,5] propose that this scale is composed of suboxides such as WO_2, $W_{18}O_{49}$, WO_3, or a sequence of these forms. Others[6] believe that the scale could be composed of WO_3 but is protective due to structural perfection or orientation. Still others[4] propose that the oxidation kinetics in the low temperature regions could be controlled by equilibria involving the physical adsorption, chemical adsorption and incorporation of oxygen. Although the mechanism controlling oxidation in the low temperature region is not confirmed, it is generally agreed that extended exposure above approximately 700° C causes a porous outer scale to develop. The large volume expansion of approximately 3.25 times, which accompanies the formation of tungsten oxide, causes the scale to crack[5]. The scale then becomes nonprotective and linear oxidation kinetics follow. The transition from parabolic to linear behavior depends upon temperature, time, and oxygen partial pressure. In addition, tungsten loss can occur due to volatility. The work of Schissel and Trulson[7] illustrated in Figure 1 shows evaporated species measured during tungsten exposures at various temperatures and in $2x10^{-4}$ torr of oxygen. Volatility of WO_3, or its polymers, is reported[8] to become noticeable at 850° C. Significant loss occurs at temperatures above 1000° C. Changes in sample weight therefore become complexly dependent upon temperature, oxygen pressure and flow conditions. For example, samples are shown in Figure 2 to lose weight at 1050° C in oxygen at less than 0.0066 atm., but to gain weight at this same temperature with 0.0066 to 0.1 atm oxygen[9]. At temperatures of greater than 1200° C the rate of WO_3 evaporation becomes equal to the rate of its formation in air[4,10] and can prevent the accumulation of oxidation products.

Ong and Fassell[3] have presented a rather extensive review of investigations into the behavior and oxidation rates of tungsten in oxygen environments. These authors have also developed Eq. 1 which represents experimental rates within a factor of two for

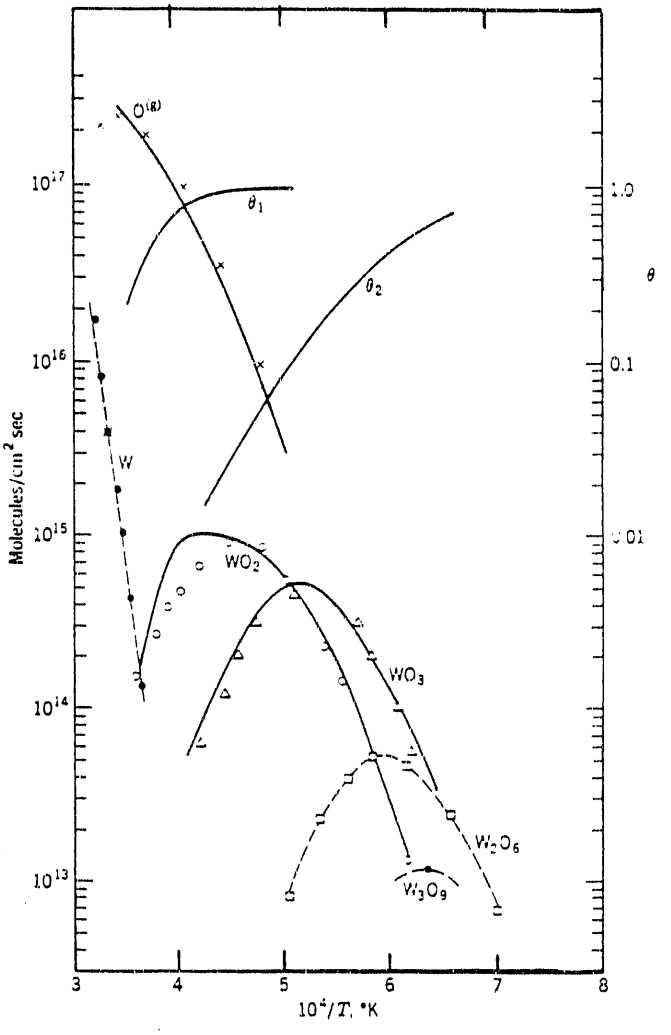

Figure 1. Evaporation rates of different gaseous species during oxidation of tungsten at 2 x 10^{-4} torr O_2 as a function of 1/T. Reference [7].

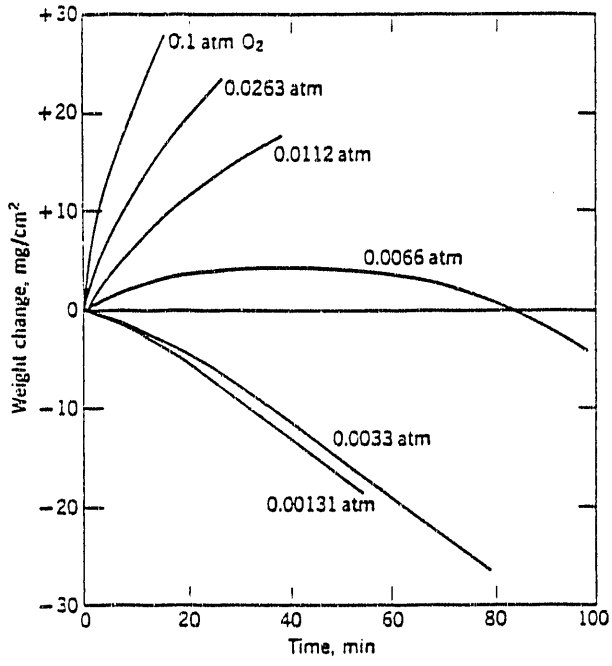

Figure 2. Oxidation of tungsten at 1050°C in various oxygen pressures. Gulbransen et al. [9].

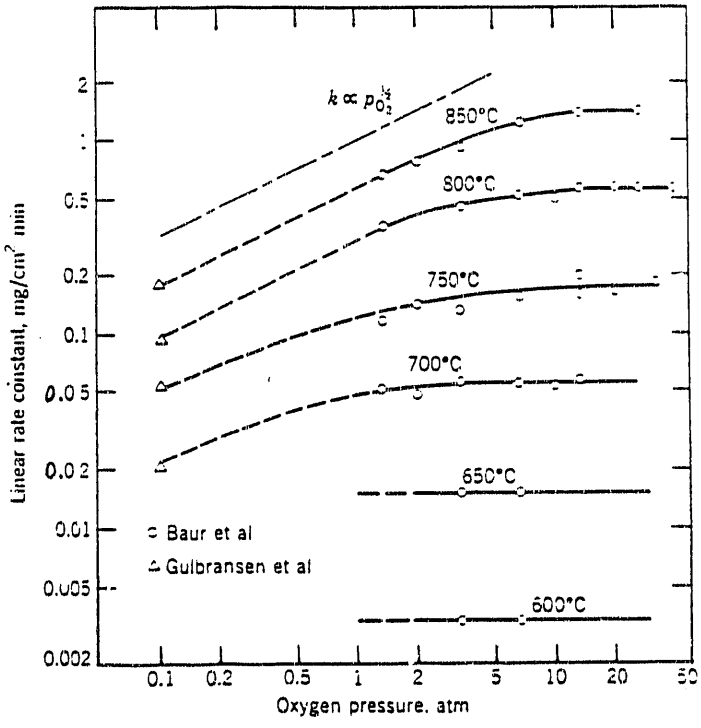

Figure 3 Linear rate constant for tungsten oxidation as a function of oxygen pressure. After Baur et al. [8] and Gulbransen et al. [9].

temperatures ranging from 700°C to 1300°C and oxygen pressures ranging from 0.0013 atm to 20.8 atm [11,12].

$$dx/dt\,(mm/s) = 0.847\ e^{-12{,}170/T}\ P_{O_2}^{\frac{1}{2}} \qquad (1)$$

The conditions encompassed in this study appear to be the ones most likely experienced in accident scenarios for fusion reactors.

Kofstad[4] also reported on work performed on the oxidation behavior of tungsten at temperatures ranging from 600°C to 850°C and oxygen pressures from 0.1 to 30 atmospheres (see Figure 3). Linear rates were observed after initial parabolic behavior. The linear rate constants were dependent upon oxygen pressure for temperatures greater than 700°C and at oxygen pressures below one atmosphere. The rate constants were proportional to the square root of the oxygen pressure. The linear rate constants were not dependent upon pressure at lower temperatures. This insensitivity to pressure also existed at higher temperatures when pressures were greater than one to five atmospheres. The relationship (Eq. 2) that the author has reported for the linear rate constant, κ_{lin} in terms of mg/cm^2-min, could be applicable for the lowest temperature, ambient pressure conditions in a fusion reactor accident. R is 1.98 cal/mole-K.

$$\kappa_{lin}\ (mg/cm^2\text{-min}) = 1.05x10^{-11}\ e^{-47{,}500/RT} \qquad (2)$$

It is well recognized that tungsten exposed to environments containing water vapor will form complex compounds which will enhance volatilization [10,13-17]. Evaporation of the tungsten species is thus dependent upon the availability of water molecules. Hastie's review of prior work[13] by Glemser and Wendlandt[14] shows linear relations between apparent WO_3 and water vapor pressure in Figure 4. This temperature range, 900°C to 1100°C, and pressures of 0 to 600 torr represent areas of interest for fusion safety evaluations. The linear plots along with the detection of some $WO_2(OH)_2$, which decomposes at lower temperatures, indicate that the vaporization process proceeds by Eq. 3.

$$WO_3(s) + H_2O = WO_2(OH)_2\ (g) \qquad (3)$$

The reaction of tungsten in water vapor as studied by Battles et al.[16] covered temperatures from 1050°C to 1275°C. Their investigation included influences of H_2O and H_2. Volatilization increased with higher H_2O to H_2 pressure ratios. The volatilization rates they reported, based upon weight change measurements, were $10x10^{-3}$ mg/cm^2-s ($5.1x10^{-7}$ mm/s) at 1200°C and $4x10^{-3}$ mg/cm^2-s ($2.1x10^{-6}$ mm/s) at 1125°C. They also reported a two-fold increase in volatilization at 1125°C as the flow rate was increased from 0.6 to 3.0 liters/minute. The preceding data were taken at 1.3 liters/minute. Assumptions by Battles, et al. are that the volatilized species is an

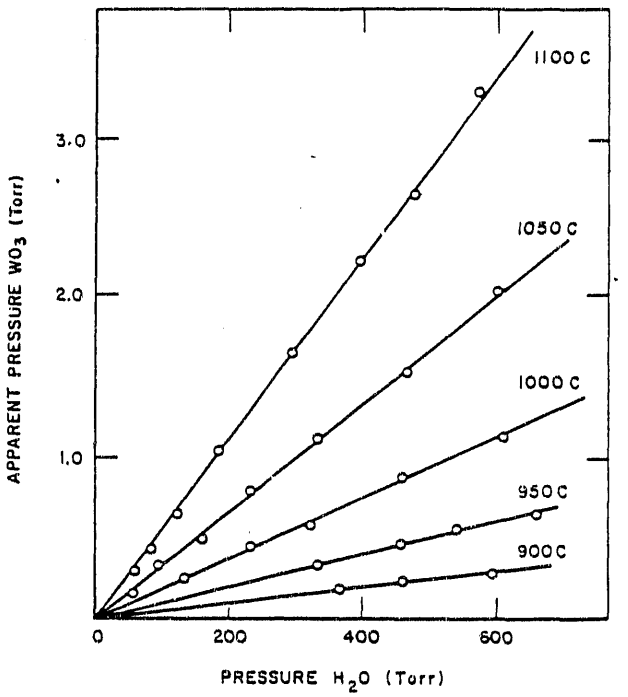

Figure 4 Isotherms of apparent vapor pressure of WO_3 as a function of water vapor pressure. Hastie's[13] review of work by Glemser and Wendlandt[14].

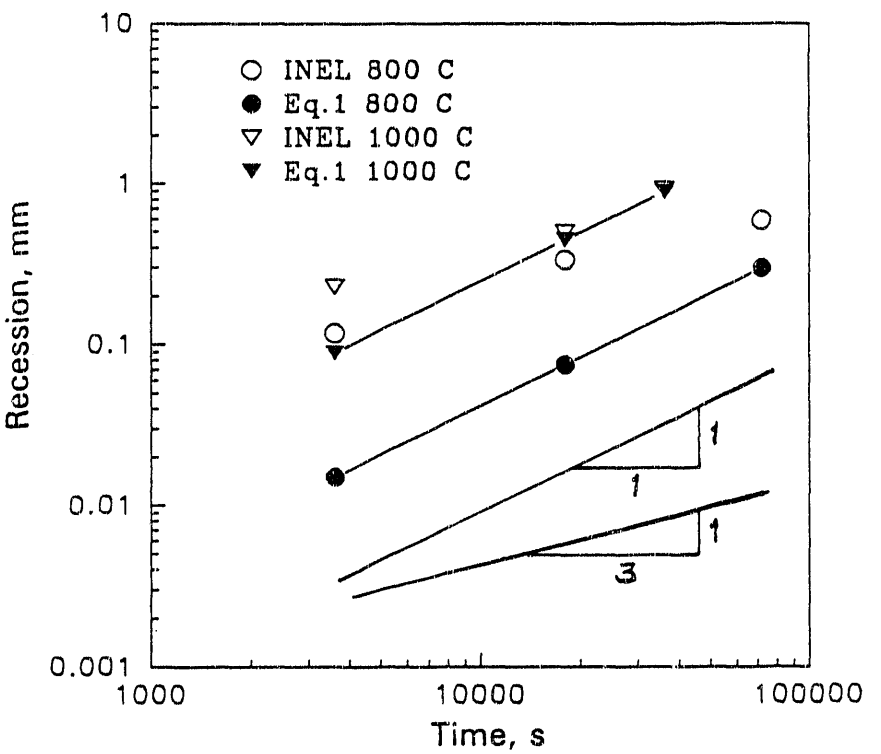

Figure 5 Recession rates of tungsten in air measured at the INEL and expressed by Eq. 1 from Ong and Fassell[11,12]. Superimposed slopes show linear and cubic oxidation behavior.

oxide-water complex having the stoichiometric formula $WO_3{*}H_2O$ and that oxide products do not accumulate on the specimen. The following reactions present several possible paths for the formation of such a species and for hydrogen generation. These authors believe that the formation of the $WO_3{*}H_2O$ complex is the rate controlling mechanism and its release as a vapor phase is rapid.

$$W + 3\,H_2O = WO_3(s) + 3H_2(g)$$
$$WO_3(s) + H_2O = WO_3{*}H_2O(g) \qquad (4a)$$

$$W + 4\,H_2O = WO_3{*}H_2O(g) + 3\,H_2(g) \qquad (4b)$$

$$W + 2\,H_2O = WO_2(s) + 2\,H_2(g) \qquad (5a)$$

$$WO_2(s) + 2\,H_2O = WO_3{*}H_2O(g) + H_2(g) \qquad (5b)$$

$$W + H_2O = WO(s) + H_2(g) \qquad (6a)$$

$$WO(s) + 3H_2O = WO_3{*}H_2O(g) + 2H_2(g) \qquad (6b)$$

The formation of residual WO_3 and other suboxides and their influence upon weight change, however, had not been considered. Hydrogen generation shown by Equations 4(a) and 4(b) indicate that three molar volumes of hydrogen is generated for each mole of WO_3 or $WO_3{*}H_2O$ formed. Each mole of WO or WO_2 will form one or two molar volumes of hydrogen, respectively. The fraction of these suboxides which transforms into $WO_3{*}H_2O$ will result in the generation of three molar volume of hydrogen. The quantity of hydrogen generated will therefore vary between the factor of one to three depending upon how much of any given suboxide forms and remains on the sample.

Volatilization losses have also been reported[17] for tungsten at temperatures above 2000°C and at vapor pressures below 10^{-4} atm. These are conditions relevant for incandescent lamp filaments. Rates reported for these conditions represented losses of around $1x10^{-5}$ g/cm^2 s, or $5.2x10^{-6}$ mm/s.

4. EXPERIMENTAL RESULTS (AIR AND STEAM TESTS)

4.1 Air Tests

Tungsten alloy samples were prepared at the INEL and tested in the VAPOR (Volatilization of Activation Product Oxides Behavior) system as previously described[1,2]. The composition of the alloy was as follows:

Table 1. Tungsten alloy composition. wt. %

W	Re	Ta	Ni	Fe	Co	Os	Cu	Mn
95	1.1	0.15	2.3	1.0	0.55	0.06	0.05	0.05

The tests environments, either air at 2 liters per minute or a 50% steam:50% argon mixture at 4 liters per minute, were flowed upward past inductively heated specimens. Specimens were exposed between 600°C to 1200°C for times varying between 15 minutes and 20 hours. Posttest evaluations included chemical analyses for volatilized constituents. These results have been reported elsewhere[1,2]. We have determined recession rates from initial sample measurements and nonreacted sample cores revealed by metallographic sections of tested specimens. Weight changes have also been obtained. We then calculated amounts of tungsten reacted from mass balances using weight change and volatilized tungsten measurements. The mass balances were based upon the following derivations:

$$\Delta M_S = \Delta M_S^O - \Delta M_V^W , \tag{7}$$

where ΔM_S is the measured sample weight change, ΔM_S^O is the amount of oxygen pickup on the sample due to oxide formation, and ΔM_V^W is the measured quantity of tungsten volatilized. The total amount of tungsten reacted is represented by:

$$\begin{aligned} \Delta M_T^W &= \Delta M_V^W + \Delta M_s^W , \ or \\ \Delta M_T^W &= \Delta M_V^W + 184/48(\Delta M_S^O) , \end{aligned} \tag{8}$$

where ΔM_T^W represents the total tungsten reacted and ΔM_S^W is the reacted tungsten which remains on the specimen. Combining Eq. 7 and Eq. 8 provides:

$$\Delta M_T^W = \Delta M_V^W + 184/48(\Delta M_S + \Delta M_V^W) . \quad (9)$$

The fraction in the last term of Eq. 9 can also be selected to consider WO or WO_2. Comparison between results from these mass balances and measured recession rates can then provide some insight into the oxide form which remains on the specimen, and also, the quantity of hydrogen generated.

The test conditions and measured recession rates for samples tested at the INEL are listed in Table 2. Predictions by Ong and Fassell[11,12], Eq.1, and Kofstad[4], Eq. 2, for the recession of tungsten in air are included along with some calculations of the amount of material reacted from weight change and volatilization measurements. The uncertainty of our recession measurements is likely about ± 0.02 mm. The measurement at 600° C is therefore probably not significant. The prediction by Eq. 1 is about ten times higher than the one by Eq. 2 at 600° C but agrees well with our weight loss calculation. Our experimental measurements are higher than Eq. 1 or Eq. 2 predictions at 800° C and for the 1-hour test at 1000° C. However, at all other high temperature conditions there seems to be a fairly good correlation between our data and Eq.1. The trends in our experimentally measured material loses are shown on a log-log plot with respect to time in Figure 5. Our tests performed at 800° C and 1000° C have a slope of approximately one-third as shown by the line included on the plot. We reported[1] similar trends for weight gain, g/cm^2. The predictions from Eq. 1 show a slope of unity for linear oxidation rates. The measured recession rates for tungsten in air from Table 2 are also plotted on an Arrhenius plot in Figure 6. Our data has been exponentially fit to two cases. One case includes mostly short-term data, i.e., 1-hour tests shown by the open circles. The other fit includes all data points. There is no significant difference between the fit for the two data sets. A plot for Eq. 1 is also included. Although the 800° C data show marked deviations from all exponential fits, Eq. 1 shows a good match with the data at higher and lower temperatures.

Sections of the oxides which formed on the tungsten alloy in air at 600, 800, and 1000° C are shown in Figure 7. All of the scales contain a fair amount of porosity and cracks which extend perpendicularly through the scale. Much of the porosity is chevron shaped, probably due to the deformation needed to accommodate the volumetric expansion of the oxide. These thick scales are not representative of a protective type of oxide which produces continually decreasing oxidation rates. They are typical of scales having linear growth rate behavior. The lower time dependence shown by the cubic relationship is therefore caused by something other than a dense impervious oxide. An abundance of voids or porosity acting as barriers can sometimes hamper the inward diffusion of oxidant species through an oxide scale. We also do not have thermal equilibrium conditions across the oxide scale. Internally the samples are hot but the gas flowing past the outer oxide surfaces is much cooler. Temperature measurements of the outer oxide surface with infrared pyrometry decrease with time as the scale grows in thickness. The driving force for oxygen diffusion into the scale is likely not only

Table 2 Test Conditions, Measurements and Predictions for Tungsten Oxidation

Specimen	Temp., °C	Time, s	Measured Surface Recession, mm	Rate of Loss, mm/s	Alloy Reacted: From Mass Balance*, mm	Predicted Metal Reacted, mm Eq. 1 [11]	Predicted Metal Reacted, mm Eq. 2 [4]
Air:							
6G	600	72,000	0.011	1.5E-7	0.027	0.022	0.0019
9G	800	3,600	0.118	3.3E-5	0.101	0.015	0.016
10G	800	18,000	0.334	1.9E-5	0.270	0.075	0.080
8G	800	72,000	0.592	8.2E-6	0.439	0.298	0.320
11G	1000	3,600	0.229	6.4E-5	0.241	0.089	---
7G	1000	18,000	0.494	2.7E-5	0.432	0.443	---
12G	1000	36,000	0.925	2.6E-5	0.612	0.886	---
13G	1200	3,600	0.240	6.7E-5	0.338	0.324	---
Steam:							
23G	600	72,000	0.009	1.2E-7	0.006	---	---
22G	800	3,600	0.019	5.3E-6	0.004	---	---
21G	800	18,000	0.058	3.2E-6	0.020	---	---
20G	800	72,000	0.079	1.1E-6	0.072	---	---
18G	1000	3,600	0.043	1.2E-5	---	---	---
15G	1000	18,000	0.198	1.1E-5	0.234	---	---
16G	1000	72,000	0.362	5.1E-6	0.600	---	---
19G	1100	2,700	0.111	4.1E-5	0.089	---	---
14G	1140	1,800	0.432	2.4E-4	0.792	---	---
24G	1200	900	0.252	2.8E-4	0.351	---	---

* The calculations from mass balances assume that WO_3 is the residual oxide from air exposures and that WO is the residual oxide from steam exposures.

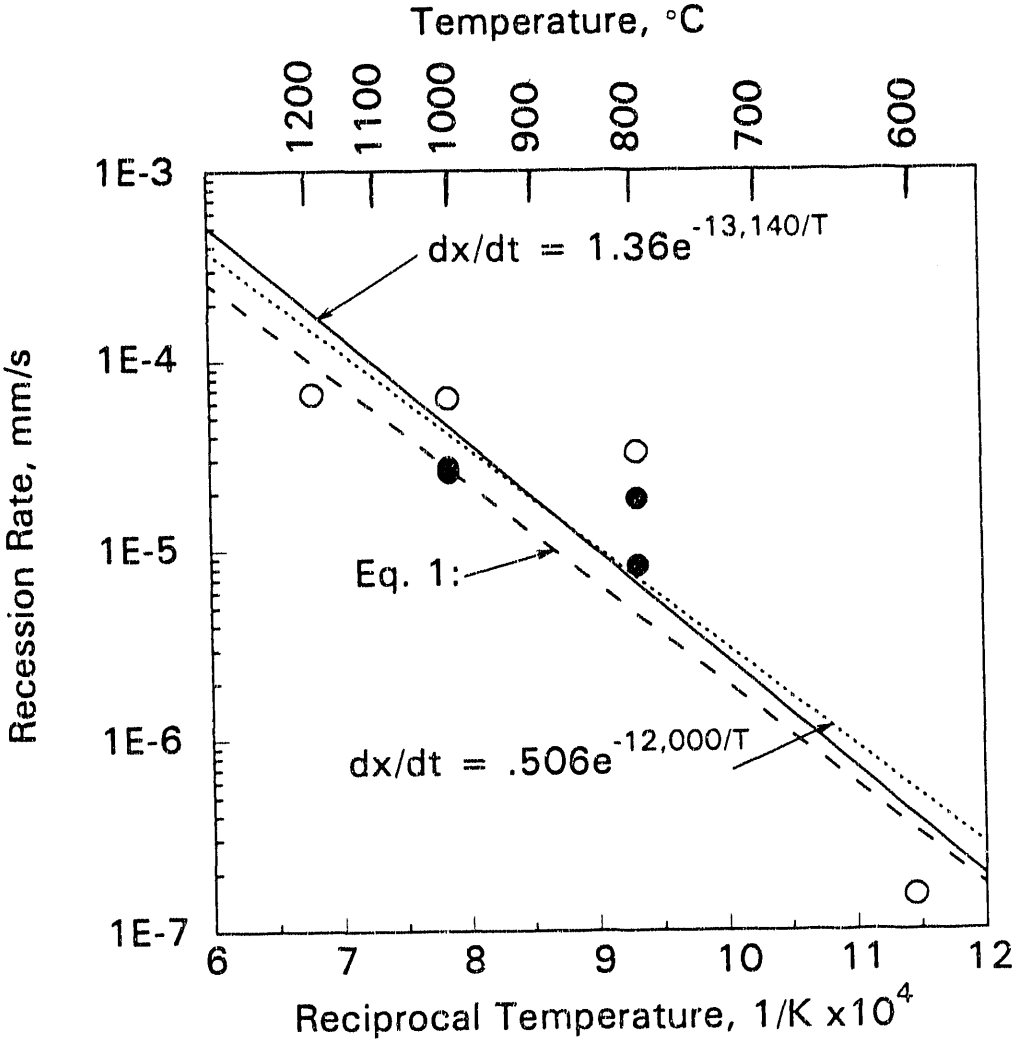

Figure 6. Exponential fits of oxidation rates of tungsten alloy in air on Arrhenius plot. INEL short term tests: open circles (solid line). INEL all data points: filled circles (dotted line). Eq. 1: Ong and Fassell[11,12] (dashed line).

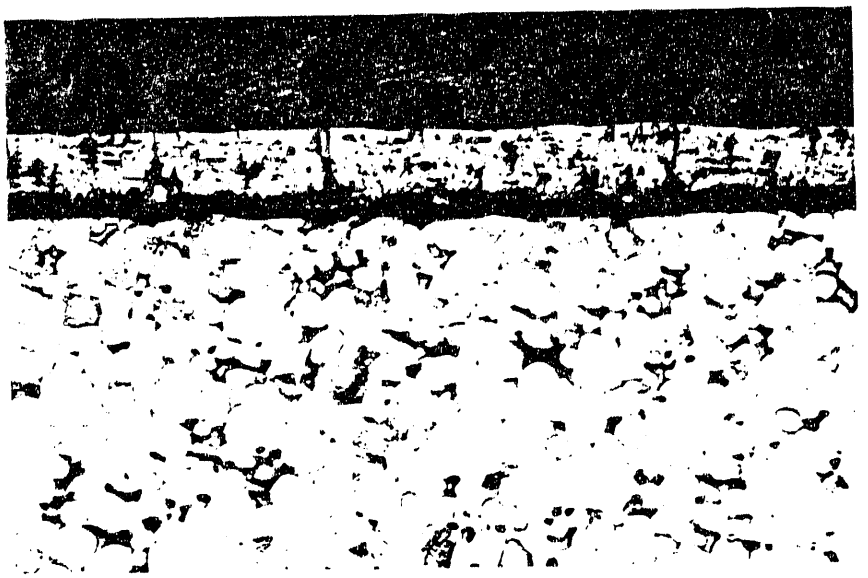

(a)

(b)

(c)

All magnifications: 100X

0.25mm

Figure 7. Sections of oxide scales formed on tungsen alloy exposed in air: (a) 600°C for 20 hours, (b) 800°C for 1 hour, (c) 1000°C for 1 hour.

dependent upon differences in chemical activity but also influenced by the temperature gradient. Adsorption and incorporation of oxygen at the outer locations may also be influenced by temperature.

Nonequilibrium conditions are likely responsible for the lower time dependence, i.e., the slope of one-third, shown in Figure 5 compared to linear behavior generally reported for tungsten oxidation in air. However, our oxidation rates are initially much higher than predicted values at 800°C and 1000°C. A better supply of oxygen due to the flow conditions in our tests compared to other investigations could cause higher initial reaction rates. This effect would then be decreased and offset as the oxide scale grows, the outer surface temperature decreases, and oxygen supply becomes more limited as discussed above.

The 800°C data looks suspiciously close to the 1000°C data. We used only infrared pyrometry for temperature measurement. This may be a reason to question temperature control, however, systematic increases in rhenium releases with time and temperature[1] provide support to our temperature measurements. We actually have insufficient data to establish oxidation relationships (see Figure 6). Additional data may show that there are two linear regions on the Arrhenius plot similar to the behavior which we have reported for beryllium[18]. Additional air tests using thermocouples would confirm temperature control and check for the possibility of two distinct regions, i.e, exponential relationships, on the Arrhenius plot. Equation 1 predictions, on the other hand, merge with our data at longer times at 800°C. Convergence within a factor of two occurs after 20 hours. I recommend using Eq. 1 to represent reaction rates at the current time. Future tests which confirm higher short-term rates near 800°C, however, would support an influence of flowing environments. Such tests may also provide us with a better idea of what is needed to adequately characterize short-term oxidation rates under nonequilibrium conditions associated with different flow rate conditions.

Another item of interest from the oxide sections, Figure 7, is the regular advancing interface at the oxide-to-alloy interface. There is no interparticle penetration. The alloy in Figure 8 shows a spherical phase at higher magnification which is basically 95% tungsten with less than 5% iron and nickel. The interparticle phase is typically composed of 50% nickel, 20% iron, 22% tungsten, 5% copper, 2% cobalt, and 1% manganese. The regular attack at the interface shows that the oxidation process is not affected by compositional and structural differences. This indicates that we should be able to make comparisons with previous investigations on the oxidation behavior of pure tungsten. Constituents spiked into the alloy should also be incorporated into the oxide scale as predicted by oxidation rates, unless preferential diffusion of a particular element within the alloy has occurred. An interesting exercise might be to perform bulk chemical analyses of oxide scale. Mass balances could then be performed for the various elements as another check for our volatility measurements.

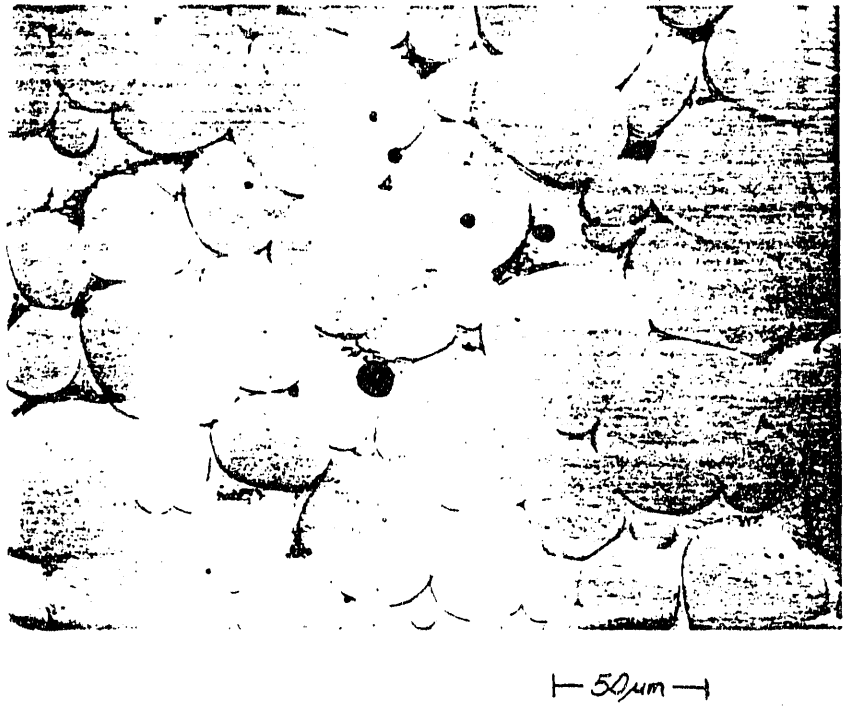

Figure 8. Microstructure of tungsten alloy showing spherical predominantly tungsten phase and interparticle phase. 400X.

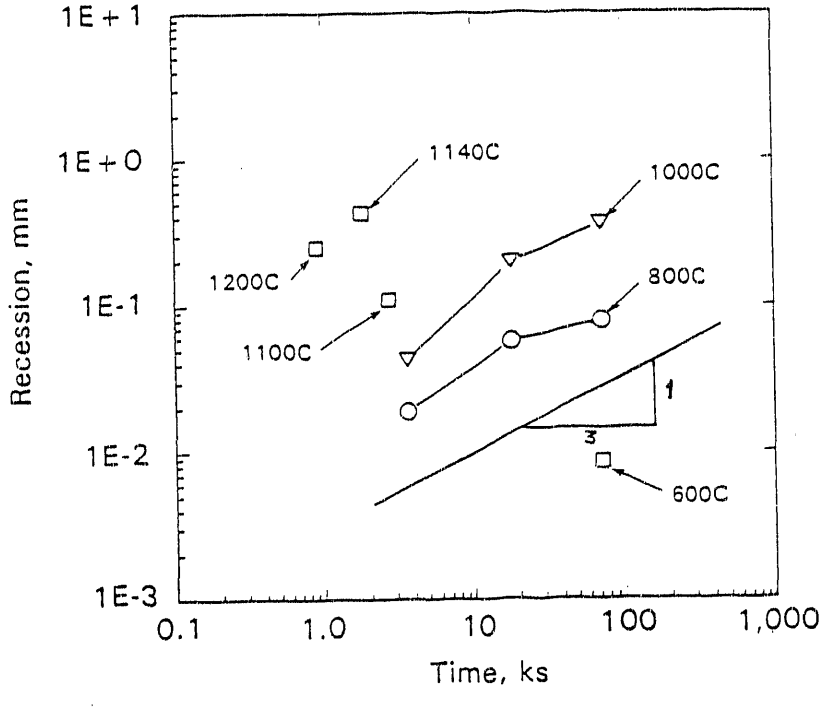

Figure 9. Log-log plot showing the extent of attack into the tungsten alloy in steam at various temperatures.

Calculations of the amount of tungsten reacted from weight change and volatilization measurement assuming residual WO_3, WO_2, or WO are listed in Table 3. There is generally good agreement between values calculated assuming WO_3 formation and measured recession rates. The exceptions are for samples which have undergone the most extensive oxidation. For these cases, better agreement tends toward the calculations assuming residual WO_2. This suggests that for thick oxide scales oxygen deficiency at inner locations may be causing WO_2 formation.

4.2 Steam Tests

The recession rates for tungsten tests in steam are plotted on a log-log plot with time in Figure 9. We again observe rates at 800°C and 1000°C which are approximated by a slope of one-third. The recession rates reported by Battles, et al.[16] for 1200°C and 1125°C were 5.1×10^{-6} mm/s and 2.1×10^{-6} mm/s, respectively. These rates are about two orders of magnitude lower than the ones we show for comparable temperatures in Table 2. These differences could be due to the higher flow rate for our experiments, i.e., 4 liters/minute compared to 1.3 liters/minutes, or due to a higher water vapor to hydrogen ratio. The ratio of these two gases would be greater than 400 in our experiments compared to 3 in the experiments by Battles, et al.
The rates reported by Harvey[17] for tungsten at higher temperatures, but lower water vapor pressures, i.e., 5.2×10^{-6} mm/s are comparable to the rates we obtained near 800°C and 1000°C.

Since the literature provides such little basis for oxidation rates in steam, I have plotted the recession rates from our short-term (1-hour) tests, plus the rate for the 20-hour 600°C test, with respect to reciprocal temperature in Figure 10. These data were fit to Eq. 10 with a coefficient of determination r^2 of 0.939. I recommend this relationship for representing oxidation rates in steam between 600°C and 1200°C. Certainly, future efforts are needed to refine the influences of flow rates and water vapor pressures.

$$dx/dt(mm/s) = 7.0\, e^{-15{,}600/T} \qquad (10)$$

Comparison between our steam and air tests indicate that oxidation rates in steam are at least less than one-half those in air below 1000°C. Above this temperature the rate of attack in steam becomes significantly higher than in air. The occurrence of vapor phase transport, as evident by dendritic or acicular shaped crystals which formed on a thin oxide layer, became apparent for samples exposed at 800°C. The extent of such crystal growth increased with time at 1000°C and provided extensive coverage at 1200°C. The accumulation of this product, rather than complete removal as referenced in the literature, could again be due to our cooler gas stream. Cooler locations on the crystal formations would provide sites for the recondensation of volatilized products. The chemical analyses of the solutions prepared from the VAPOR apparatus confirmed that significant amounts of tungsten compounds had volatilized at the higher temperatures.

Table 3 Recession Measurements and Calculations for Tungsten Specimens

Specimen	Temp., °C	Time, s	Measured Surface Recession, mm	Calculated Losses With WO_3, mm	Calculated Losses With WO_2, mm	Calculated Losses With WO, mm
Air:						
6G	600	72,000	0.011	0.027	0.041	0.081
9G	800	3,600	0.118	0.101	0.152	0.303
10G	800	18,000	0.334	0.270	0.402	0.815
8G	800	72,000	0.592	0.439	0.658	1.297
11G	1000	3,600	0.229	0.241	0.362	0.723
7G	1000	18,000	0.494	0.432	0.653	1.306
12G	1000	36,000	0.925	0.612	0.918	1.875
13G	1200	3,600	0.240	0.338	0.507	0.994
Steam:						
23G	600	72,000	0.009	0.002	0.003	0.006
22G	800	3,600	0.019	0.002	0.002	0.004
21G	800	18,000	0.058	0.009	0.011	0.020
20G	800	72,000	0.079	0.027	0.039	0.072
18G	1000	3,600	0.043	---	---	----
15G	1000	18,000	0.198	0.090	0.124	0.234
16G	1000	72,000	0.362	0.220	0.320	0.600
19G	1100	2,700	0.111	0.050	0.062	0.089
14G	1140	1,800	0.432	0.297	0.426	0.792
24G	1200	900	0.252	0.145	0.198	0.351

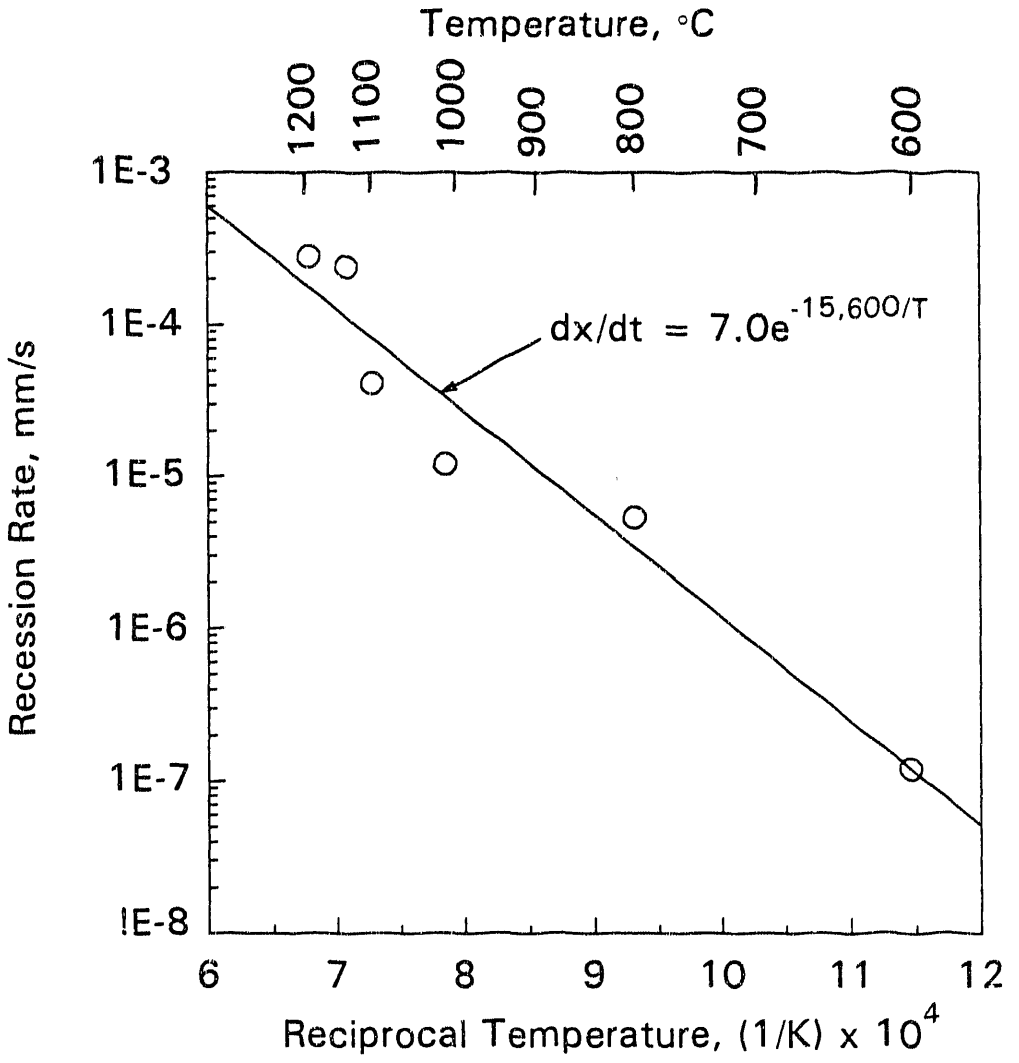

Figure 10. Arrhenius plot and recession rate relationship derived for the tungsten alloy tests performed in steam at the INEL.

Calculations of reacted tungsten based upon weight change and volatility losses (see Table 3) suggest that remnant oxides could consist of WO and WO_2. The formation of WO seems favored at or below 800°C and also for shorter term tests at higher temperatures. However, for tests which have undergone more extensive oxidation due to higher temperatures, or longer times, the existence of WO_2, or a mixture of WO and WO_2 seems to provide the best agreement. The formation of these oxides of lower oxidation states in steam compared to WO_3 in air agrees with the fact that the steam environments have lower oxygen activities. A conservatively high estimate of hydrogen production would be to assume that three molar volumes of hydrogen are produced for every mole of tungsten reacted. Equation 10 can then be multiplied by 0.70 to express liters of H_2/cm^2-s.

5. COMPARISON OF HYDROGEN GENERATION RATES

The relative rates for hydrogen generation by the three candidate materials; beryllium, graphite and tungsten exposed in steam are shown for temperatures ranging from 600°C to 1700°C in Figure 11. This information, including that for beryllium and graphite[18,19,20] has been normalized to show the rate of hydrogen generated per unit area, liters/m^2-s. Steam input and surface velocities were different for the tests on these materials. Graphite was tested with the highest steam input of 0.42 liters/s which provided a velocity of 6.6 m/s at the surface. Steam input and surface velocity were 0.21 liters/s and 0.26 m/s, respectively, for beryllium. Tungsten tests had the lowest input of 0.04 liters/s and the lowest surface velocities of 0.1 m/s. We observed[20] a linear scaling of the reaction rate of graphite with steam pressure above 1300°C. The upper portion of the graphite curve in Figure 11 would therefore be lowered about one order of magnitude for a steam input comparable to that used for tungsten. This would decrease hydrogen generation rates to less than those shown for tungsten. I would also expect the hydrogen generation rate of tungsten to increase relative to that of beryllium, but remain less, at comparable steam supplies. In summary, the rates for hydrogen generation at a particular temperature increase in the order of graphite, tungsten, and then beryllium. Unfortunately, each of these materials also has detrimental attributes. Graphite develops high tritium inventories and has high erosion rates. Tungsten has the potential for high activation products releases due to the high volatility of oxide-hydroxide species. Beryllium reacts rapidly in steam and produces toxic BeO particulate.

The total quantity of hydrogen produced during an accident involving PFCs based upon graphite, tungsten, or beryllium technology depends upon the specific design and operating parameters. For example, graphite tiles are expected to be operated at temperatures of 1000°C to 1800°C. We have calculated[19,20] the quantities of hydrogen produced from such tiles during short-term (~5 minute) transients due to in-vessel loss of coolant accidents (LOCAs). This helped establish the fraction of tiles which could be operated at particular temperatures to remain below a 10 kg limit for hydrogen generation. Tungsten or beryllium coated tiles would be conductively cooled and

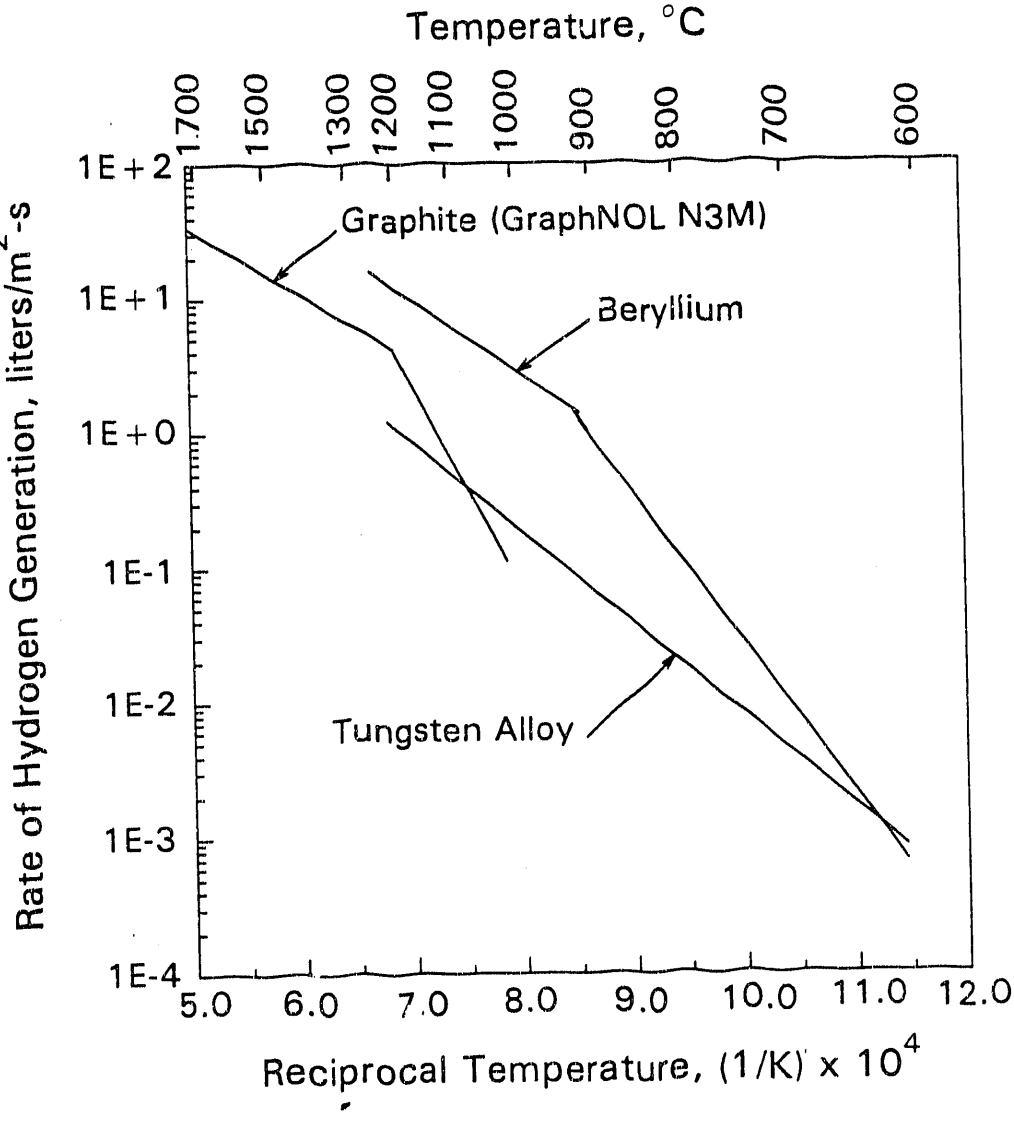

Figure 11. Rates of hydrogen production by the reactions of graphite, beryllium and tungsten with steam. Obtained from the current report and references 18 and 19.

Hydrogen Generation Rates, liters H_2/m^2-s

Beryllium:	873 K ≤ T ≤ 1173 K,	Rate = $4.8 \times 10^9 e^{-25,850/T}$
	1173 K ≤ T ≤ 1473 K,	Rate = $7.9 \times 10^4 e^{-12,830/T}$
GraphNOL N3M:	1273 K ≤ T ≤ 1460 K,	Rate = $1.6 \times 10^{11} e^{-35,630/T}$
	1460 K ≤ T ≤ 2000 K,	Rate = $9.7 \times 10^3 e^{-11,320/T}$
Tungsten:	873 K ≤ T ≤ 1473 K,	Rate = $4.9 \times 10^4 e^{-15,600/T}$

operated between 600°C to 800°C. The concern for these materials from a LOCA is the reaction with steam and resultant hydrogen production during the 3 to 4 week long temperature excursion due to decay heating following a LOCA. The utility of the information shown in Figure 11 is that it is currently the best, although not complete, representation for the reaction of these materials in steam. They are the reaction rates I would recommend for use in safety analyses for different fusion reactor designs and accident scenarios as they are required. In particular, these rates will be used in the development of a PFC safety assessment tool. This tool, which is under development at the INEL, will give hydrogen production, chemical energy released, and activation product dose (including beryllium toxicity) as a function of several PFC materials, and whether the accident involves air or steam for various heat sink and heat transport assumptions.

Acknowledgements

I wish to acknowledge my following associates for their contributions to this investigation: George Reimann and Barry Rabin for assistance in alloy development, Ron Wallace for performing the tests, Kyle Messick and Ed McNew for developing procedures and performing chemical analyses, Vonda Smith-Wackerle and Gary Fletcher for performing the optical metallography, and Del Miley for examinations by scanning electron microscopy.

6. REFERENCES

1. G. R. Smolik, R. M. Neilson, Jr., and S. J. Piet, "Volatility from Copper and Tungsten Alloys for Fusion Reactor Applications," 13th IEEE Symposium on Fusion Engineering, Knoxville, TN, October 2-3, 1989. pp. 670-673.

2. G. R. Smolik, S. J. Piet, and R. M. Neilson, Jr., "Predictions of Radioactive Tungsten Release from Hypothetical ITER Accidents", *Fusion Technology*, 19, (No.3, Part 2B), May 1991, pp. 1398-1402.

3. J. N. Ong, Jr. and W. M. Fassell, Jr., "Effects of Alloying Elements on the Oxidation of Refractory Metals", in *Refractory Metals and Alloys II*, ed. by M. Semchyshen and I. Perlmutter, Interscience Publishers, 1962, pp. 223-268.

4. P. Kofstad, *High Temperature Oxidation of Metals*, John Wiley & Sons, Inc., 1966, pp. 251-260.

5. O. Kubaschewski and B. E. Hopkins, "Oxidation Mechanism of Niobium, Tantalum, Molybdenum, and Tungsten" in Conference held at The University of Sheffield, September 20-22, 1960, ed. A. G. Quarrell, 1961, pp. 181-189.

6. E. A. Kellet and S. E. Rogers, "The Structure of Oxide Layers on Tungsten," *J. Electrochemical Soc.*, 110, 1963, pp.502-504.

7. P. O. Schissel and O. C. Trulson, "Mass-Spectrometric Study of the Oxidation of Tungsten," *J. Chem. Phys.*, 43, 1965, pp. 737-743.

8. J. P. Baur, D. W. Bridges and W. M. Fassell, "High Pressure Oxidation of Metals - Tungsten in Oxygen," *J. Electrochem. Soc.* 103, 1956, pp. 266-272.

9. E. A Gulbransen, K. F. Andrew, P. E. Blackburn, T. P. Copan and A. Merlin, "Oxidation of Tungsten and Tungsten Based Alloys," WADC Tech. Rept. 59-575, 1962.

10. S. Mrowec and T. Weber, *Gas Corrosion of Metals*, National Bureau of Standards and the National Science Foundation, NTIS-TT 76-54038, 1978, p. 411.

11. J. N. Ong, Jr. "Oxidation of Refractory Metals as a Function of Pressure, Temperature, and Time: Tungsten in Oxygen", *J. Electrochem. Soc.*, 109, No. 4, 1962, pp. 284-288.

12. J. N. Ong, Jr. and W. M. Fassell, Jr., "Kinetics of Oxidation of Columbian and Other Refractory Metals", *Corrosion*, 18, 1962, pp. 382t-389t.

13. J. W. Hastie, *High Temperature Vapors*, Academic Press, New York, N. Y., 1975, pp. 62-68.

14. O. Glemser and H. G. Wendlandt, "Gaseous Hydroxides," *Advan. Inorg. Chem. Radiochem.*, 5, 1963, pp. 215-258.

15. R. Speiser and G. R. St. Pierre, *The Science and Technology of Tungsten, Tantalum, Molybdenum, Niobium, and Their Alloys*, ed. by N. E. Promisel, Pregamon Press, London, 1964, p. 289.

16. J. E. Battles, G. R. St. Pierre, and R. Speiser, "Reaction of Water Vapor and Tungsten", *Metallurgie*, 7, No. 2, 1967, pp. 69-77.

17. F. J. Harvey, "High Temperature Oxidation Of Tungsten Wires in Water Vapor-Argon Mixtures," *Met. Trans.*, 5, May 1974, pp. 1189-1192.

18. G. R. Smolik, B. J. Merrill, and R. S. Wallace, "Implications of Beryllium:Steam Interactions in Fusion Reactors", Fifth International Conference on Fusion Reactor Materials, Clearwater, FL, November 17-22, 1991.

19. G. R. Smolik, B. J. Merrill, S. J. Piet, D. F. Holland, "Evaluation of Graphite/Steam Interactions for ITER Accident Scenarios", *Fusion Technology*, 19, No. 3, Part 2A, 1991, pp. 1342-1348.

20. G. R. Smolik, B. J. Merrill, S. J. Piet, D. F. Holland, "Evaluation of Graphite/Steam Interactions for ITER", EGG-FSP-9154, September, 1990.

END

DATE
FILMED
9/01/92